Exploiting Persymmetry for Adaptive Detection in Distributed MIMO Radar

Jun Liu and Hongbin Li
ECE Department, Stevens Institute of Technology
Hoboken, NJ 07030, USA
(e-mail: jun_liu_math@hotmail.com; hongbin.li@stevens.edu)

Braham Himed
RF Technology Branch, AFRL
WPAFB, OH 45433, USA
(email: braham.himed@us.af.mil)

***Abstract*—We consider the adaptive detection problem in colored Gaussian noise with unknown persymmetric covariance matrix in a multiple-input-multiple-output (MIMO) radar with spatially dispersed antennas. To this end, a set of secondary data for each transmit-receive pair is assumed to be available. MIMO versions of the persymmetric generalized likelihood ratio test (MIMO-PGLRT) detector and the persymmetric sampler matrix inversion (MIMO-PSMI) detector are proposed. Compared to the MIMO-PGLRT detector, the MIMO-PSMI detector has a simple form and is computationally more efficient. Numerical examples are provided to demonstrate that the proposed two detection algorithms can significantly alleviate the requirement of the amount of secondary data, and allow for a noticeable improvement in detection performance.**

***Index Terms*—Adaptive detection, multiple-input-multiple-output (MIMO) radar, persymmetry.**

I. Introduction

THE paradigm of multiple-input multiple-output (MIMO) which originated in communications is more and more widely applied to radars [1]. In general, MIMO radar falls into two classes according to the configuration of its antennas: one with co-located antennas [2], [3] and the other with widely distributed antennas [4], [5], [6]. We restrict ourselves to the second MIMO radar configuration, which for brevity is referred to as MIMO radar in the following.

In [7], several temporal coherent adaptive detectors are proposed to deal with the problem of target detection in MIMO radar. A set of training data is employed for each transmit-receive pair to estimate the unknown clutter covariance matrix. In [8], a MIMO version of the generalized likelihood ratio test (MIMO-GLRT) detector, which is an extension of the detector in [7, eq. (19)], is developed, and its false alarm rate is obtained in closed form. It is shown that the number of training data has a great impact on the detection performance of the MIMO radar, and the detection performance is significantly degraded when the number of training data is small. In many practical scenarios, it is difficult to collect a large number of independent identically distributed target-free training data due to many factors such as variations in terrain [9] and interfering targets [10]. Therefore, it is interesting to investigate how to achieve satisfactory detection performance when the amount of training data is limited.

Jun Liu is now with National Laboratory of Radar Signal Processing, Xidian University, Xian, 710071, China.

Some prior knowledge about the structure of clutter covariance matrix (e.g. persymmeric structure) may be exploited to alleviate the requirement of the amount of training data [11]. In practical applications, the clutter covariance matrix has a Hermitian persymmetric (also called centrohermitian) form, when a detection system is equipped with a symmetrically spaced linear array [12, chap. 7] or symmetrically spaced pulse trains [13]. Hermitian persymmetry has a property of doubly symmetry, i.e., Hermitian about its principal diagonal and persymmetric about its cross diagonal. Unless otherwise stated, "persymmetric" always denotes "Hermitian persymmetric" for brevity in the following.

The investigation on the persymmetric structure of clutter covariance matrix can be traced to Nitzberg's paper [14], where the maximum likelihood (ML) estimate of the persymmetric covariance matrix was obtained. Using this ML estimate, Cai and Wang developed two persymmetric detection algorithms, i.e., the persymmetric multiband generalized likelihood ratio test (GLRT) algorithm [13] and the persymmetric sample matrix inversion (SMI) algorithm [15]. In recent years, several other detection algorithms have been proposed with a-priori information on the persymmetric structure of the clutter covariance (see [16], [17], [18], [19], [20]). All these persmmetric detection algorithms mentioned above validate the fact that an obvious gain in detection performance can be obtained by exploiting persymmetric structures in the clutter covariance, especially when the amount of training data available is limited.

In this study, we examine the adaptive detection problem in the presence of colored Gaussian noise with unknown covariance matrix in a distributed MIMO radar, by using persymmetric structures in the received data. The unknown noise covariance matrix for each transmit-receive pair is estimated from a set of secondary data. A MIMO version of the persymmetric GLRT detector, referred to as the MIMO-PGLRT detector, is proposed. Moreover, we develop a MIMO version of the persymmetric SMI detector, referred to as the MIMO-PSMI detector, which is simpler than the former detector, and thus has lower computational complexity. Simulation results reveal that compared to the conventional MIMO-GLRT detector which do not use the persymmetric structure, both of the proposed detectors obtain significant gains in detection performance, especially when the amount of secondary data is

978-0-9928-6265-7/16/$31.00 ©2016 IEEE

limited. Additionally, the MIMO-PGLRT detector outperforms the MIMO-PSMI detector, even though a higher computational burden is incurred. However, the performance difference among these four MIMO detectors is negligible when the amount of training data is adequate.

Notation: Vectors (matrices) are denoted by boldface lower (upper) case letters. Superscripts $(\cdot)^T$, $(\cdot)^*$ and $(\cdot)^\dagger$ denote transpose, complex conjugate and complex conjugate transpose, respectively. The notation $\sim$ means "is distributed as," and $\mathcal{CN}$ denotes a circularly symmetric, complex Gaussian distribution. $\mathbf{I}_p$ stands for a p-dimensional identity matrix. $|\cdot|$ represents the modulus of a complex number and $\jmath = \sqrt{-1}$. $\det(\cdot)$ and $\mathrm{tr}(\cdot)$ denote the determinant and trace of a matrix, respectively. $\mathfrak{Re}(\cdot)$ and $\mathfrak{Im}(\cdot)$ represent the real and imaginary parts of a complex quantity, respectively.

II. Signal Model

In this section, a signal model for MIMO radar with widely distributed antennas is presented. Suppose that a MIMO radar consists of M transmit antennas and N receive antennas which are geographically dispersed. The total number of transmit-receive paths available is $V = MN$. Assume that the tth transmitter sends Q_t pulses and a target to be detected does not leave the cell under test during these pulses. We further impose the standard assumption that all transmit waveforms are orthogonal to each other, and each receiver uses a bank of M matched filters corresponding to the M orthogonal waveforms.

Sampled at the pulse rate via slow-time sampling, the signal received by the rth receive antenna due to the transmission from the tth transmit antenna, which is usually called test data (primary data), can be expressed as a $Q_t \times 1$ vector, i.e.,

$$\mathbf{x}_{r,t} = a_{r,t}\,\mathbf{s}_{r,t} + \mathbf{n}_{r,t}, \tag{1}$$

where $\mathbf{s}_{r,t} \in \mathbb{C}^{Q_t \times 1}$ denotes a known $Q_t \times 1$ steering vector for the target relative to the tth transmitter and rth receiver pair [5]; $a_{r,t} \in \mathbb{C}$ is a deterministic but unknown complex scalar accounting for the target reflectivity and the channel propagation effects in the tth transmitter and rth receiver pair; the noise $\mathbf{n}_{r,t} \sim \mathcal{CN}(\mathbf{0}, \mathbf{R}_{r,t})$, where $\mathbf{R}_{r,t}$ is a positive definite covariance matrix of dimension $Q_t \times Q_t$.

These primary data vector $\{\mathbf{x}_{r,t}\}$ can be assumed independent of each other due to the widely distributed antennas in the MIMO radar. Notice that in the above model (1), these steering vectors $\mathbf{s}_{r,t}$'s are not necessarily identical even though they describe the same target, since the relative position and velocity of the target with respect to different widely dispersed radars may be distinct. In addition, the covariance matrices $\mathbf{R}_{r,t}$'s are also not constrained to be the same, because the statistical properties of the noise may be unique for each transmit-receive perspective. We further assume that $Q_t > 1, t = 1, 2, \ldots, M$, such that coherent processing for each test data is possible. Notice that Q_t, $t = 1, 2, \ldots, M$ are not constrained to be identical, which means that the numbers of the pulses transmitted by different transmit antennas may be distinct. Another standard assumption we impose is that for each test data vector $\mathbf{x}_{r,t}$, there exists a set of training data (secondary data) free of target signal components, i.e., $\{\mathbf{y}_{r,t}(k), k = 1, 2, \ldots, K_{r,t} | \mathbf{y}_{r,t}(k) \sim \mathcal{CN}(\mathbf{0}, \mathbf{R}_{r,t})\}$. Note that the numbers of secondary data vectors $K_{r,t}$ are not constrained to be the same. Suppose further that these secondary data vectors are independent of each other and of the primary data vectors.

The detection problem considered herein involve structured $\mathbf{R}_{r,t}$ and $\mathbf{s}_{r,t}$. Specifically, it is supposed that each of the $\mathbf{R}_{r,t}$'s has the persymmetric property, i.e., $\mathbf{R}_{r,t} = \mathbf{J}\mathbf{R}_{r,t}^*\mathbf{J}$ where $\mathbf{J}$ is a permutation matrix with unit anti-diagonal elements and zeros elsewhere [19]. In addition, the steering vector is also assumed to be a persymmetric one satisfying $\mathbf{s}_{r,t} = \mathbf{J}\mathbf{s}_{r,t}^*$. The above assumption on the structures of $\mathbf{R}_{r,t}$ and $\mathbf{s}_{r,t}$ is valid when each antenna in the MIMO radar uses a pulse train symmetrically spaced with respect to its mid time delay for temporal domain processing. In the common case of pulse trains with uniform spacing, the steering vector $\mathbf{s}_{r,t}$ has the form:

$$\begin{aligned}\mathbf{s}_{r,t} \;=\; & \Big[\mathrm{e}^{-\jmath\frac{(Q_1-1)2\pi\bar{f}_{r,t}}{2}}, \ldots, \mathrm{e}^{-\jmath\, 2\pi\bar{f}_{r,t}}, 1, \\ & \mathrm{e}^{\jmath\, 2\pi\bar{f}_{r,t}}, \ldots, \mathrm{e}^{\jmath\frac{(Q_1-1)2\pi\bar{f}_{r,t}}{2}}\Big]^T,\end{aligned} \tag{2}$$

where $\bar{f}_{r,t}$ defined similarly as [5, eq. (2)] is the normalized target Doppler shift corresponding to the tth transmitter and rth receiver pair.

Let the null hypothesis (H_0) be such that the primary data is free of the target signal and the alternative hypothesis (H_1) be such that the primary data contains the target signal. Hence, the detection problem is to decide between the null hypothesis and the alternative one:

$$H_0 : \begin{cases}\mathbf{x}_{r,t} \sim \mathcal{CN}(\mathbf{0}, \mathbf{R}_{r,t}) \\ \mathbf{y}_{r,t}(k) \sim \mathcal{CN}(\mathbf{0}, \mathbf{R}_{r,t})\end{cases} \tag{3a}$$

and

$$H_1 : \begin{cases}\mathbf{x}_{r,t} \sim \mathcal{CN}(a_{r,t}\,\mathbf{s}_{r,t}, \mathbf{R}_{r,t}) \\ \mathbf{y}_{r,t}(k) \sim \mathcal{CN}(\mathbf{0}, \mathbf{R}_{r,t})\end{cases} \tag{3b}$$

for $t = 1, 2, \ldots, M$, $r = 1, 2, \cdots, N$, and $k = 1, 2, \ldots, K_{r,t}$. In [7], [8], MIMO detection algorithms were developed without using any prior knowledge about the special structure of the noise covariance matrix. In the sequel, two adaptive detectors are proposed by exploiting the persymmetric structures of $\mathbf{R}_{r,t}$ and $\mathbf{s}_{r,t}$. It will be seen that the exploitation of persrmmetry can bring in a noticeable detection gain.

III. Persymmetric Adaptive Detection

A. MIMO-PGLRT Detector

Due to the unknown parameters $a_{r,t}$ and $\mathbf{R}_{r,t}$, the Neyman-Pearson criterion can not be employed. According to the GLRT, a practical detector can be obtained by replacing all the unknown parameters with their ML estimates, i.e., the detector is obtained by

$$\frac{\max_{\{a_{r,t},\mathbf{R}_{r,t}\,|\,t=1,2,\ldots,M,\;r=1,2,\ldots,N\}} f\left(\mathbf{X}|H_1\right)}{\max_{\{\mathbf{R}_{r,t}\,|\,t=1,2,\ldots,M,\;r=1,2,\ldots,N\}} f\left(\mathbf{X}|H_0\right)} \underset{H_0}{\overset{H_1}{\gtrless}} \lambda_0, \tag{4}$$

where λ_0 is the detection threshold, $f(\cdot)$ denotes probability density function (PDF), and $\mathbf{X} = [\mathbf{X}_{1,1}, \ldots, \mathbf{X}_{N,M}]$ with $\mathbf{X}_{r,t} = [\mathbf{x}_{r,t}, \mathbf{y}_{r,t}(1), \mathbf{y}_{r,t}(2), \ldots, \mathbf{y}_{r,t}(K_{r,t})]$. Due to the independent assumption on these test data vectors, the PDF of $\mathbf{X}$ under H_q ($q = 0, 1$) can be represented as

$$f(\mathbf{X}|H_q) = \prod_{r=1}^{N}\prod_{t=1}^{M} \underbrace{f_{\mathbf{X}_{r,t}}(\mathbf{X}_{r,t}|H_q)}_{\triangleq f_{r,t,q}}, \quad q = 0, 1, \tag{5}$$

where

$$f_{r,t,q} = \left\{\frac{1}{\pi^{Q_t}\det(\mathbf{R}_{r,t})}\exp\left[-\mathrm{tr}(\mathbf{R}_{r,t}^{-1}\mathbf{T}_{r,t,q})\right]\right\}^{K_{r,t}+1} \tag{6}$$

with

$$\mathbf{T}_{r,t,q} = \frac{1}{K_{r,t}+1}\left[\sum_{k=1}^{K_{r,t}} \mathbf{y}_{r,t}(k)\mathbf{y}_{r,t}^{\dagger}(k) \right. \\ \left. + (\mathbf{x}_{r,t} - qa_{r,t}\,\mathbf{s}_{r,t})(\mathbf{x}_{r,t} - qa_{r,t}\,\mathbf{s}_{r,t})^{\dagger}\right]. \tag{7}$$

Define

$$\hat{\mathbf{R}}_{r,t} = \frac{1}{2}\sum_{k=1}^{K_{r,t}}\left\{\mathbf{y}_{r,t}(k)\mathbf{y}_{r,t}^{\dagger}(k) + \mathbf{J}[\mathbf{y}_{r,t}(k)\mathbf{y}_{r,t}^{\dagger}(k)]^{*}\mathbf{J}\right\} \tag{8}$$

$$\mathbf{x}_{r,t}^{\mathrm{e}} = \frac{1}{2}\left[(\mathbf{I}+\mathbf{J})\mathfrak{Re}(\mathbf{x}_{r,t}) - (\mathbf{I}-\mathbf{J})\mathfrak{Im}(\mathbf{x}_{r,t})\right] \tag{9}$$

$$\mathbf{x}_{r,t}^{\mathrm{o}} = \frac{1}{2}\left[(\mathbf{I}-\mathbf{J})\mathfrak{Re}(\mathbf{x}_{r,t}) + (\mathbf{I}+\mathbf{J})\mathfrak{Im}(\mathbf{x}_{r,t})\right] \tag{10}$$

and

$$\tilde{\mathbf{X}}_{r,t} = [\mathbf{x}_{r,t}^{\mathrm{e}}, \mathbf{x}_{r,t}^{\mathrm{o}}]. \tag{11}$$

As derived in Appendix A, the detector is given by

$$\prod_{r=1}^{N}\prod_{t=1}^{M}\left(\frac{1}{1-\Phi_{r,t}}\right)^{K_{r,t}+1} \underset{H_0}{\overset{H_1}{\gtrless}} \lambda_0, \tag{12}$$

where

$$\Phi_{r,t} = \frac{\tilde{\mathbf{s}}_{r,t}^{\dagger}\tilde{\mathbf{R}}_{r,t}^{-1}\tilde{\mathbf{X}}_{r,t}(\mathbf{I}_2 + \tilde{\mathbf{X}}_{r,t}^{\dagger}\tilde{\mathbf{R}}_{r,t}^{-1}\tilde{\mathbf{X}}_{r,t})^{-1}\tilde{\mathbf{X}}_{r,t}^{\dagger}\tilde{\mathbf{R}}_{r,t}^{-1}\tilde{\mathbf{s}}_{r,t}}{\tilde{\mathbf{s}}_{r,t}^{\dagger}\tilde{\mathbf{R}}_{r,t}^{-1}\tilde{\mathbf{s}}_{r,t}} \tag{13}$$

with $\tilde{\mathbf{s}}_{r,t} = \mathfrak{Re}(\mathbf{s}_{r,t}) - \mathfrak{Im}(\mathbf{s}_{r,t})$, and $\tilde{\mathbf{R}}_{r,t} = \mathfrak{Re}(\hat{\mathbf{R}}_{r,t}) + \mathbf{J}\mathfrak{Im}(\hat{\mathbf{R}}_{r,t})$. Here, (12) is referred to as the MIMO-PGLRT detector.

Notice that there exists a significant difference between the detector (13) developed in [13] and the MIMO-PGLRT detector (12) derived here. In [13], the noise covariance matrices at multiple bands are assumed to be identical, whereas in our study the noise covariance matrices at different transmit-receive pairs may be distinct.

B. MIMO-PSMI Detector

Here, an alternative solution to the detection problem (3) is proposed, which has a lower computational burden than the MIMO-PGLRT detector. To this end, an approach similar to that in [15] is employed. More specifically, for each transmit-receive pair we use the following test statistic:

$$\Xi_{r,t} = |\mathbf{w}_{r,t}^{\dagger}\mathbf{x}_{r,t}^{\mathrm{e}}|^2 + |\mathbf{w}_{r,t}^{\dagger}\mathbf{x}_{r,t}^{\mathrm{o}}|^2, \tag{14}$$

where $\mathbf{x}_{r,t}^{\mathrm{e}}$ and $\mathbf{x}_{r,t}^{\mathrm{o}}$ are defined in (9) and (10), respectively, and the weight vector $\mathbf{w}_{r,t}$ is given by

$$\mathbf{w}_{r,t} = \frac{\tilde{\mathbf{R}}_{r,t}^{-1}\tilde{\mathbf{s}}_{r,t}}{(\tilde{\mathbf{s}}_{r,t}^{\dagger}\tilde{\mathbf{R}}_{r,t}^{-1}\tilde{\mathbf{s}}_{r,t})^{1/2}}. \tag{15}$$

Jointly processing the independent data received by all the transmit-receive pairs, we have the following decision rule:

$$\Xi = \sum_{r=1}^{N}\sum_{t=1}^{M}\Xi_{r,t} = \sum_{r=1}^{N}\sum_{t=1}^{M}\frac{\tilde{\mathbf{s}}_{r,t}^{\dagger}\tilde{\mathbf{R}}_{r,t}^{-1}\tilde{\mathbf{X}}_{r,t}\tilde{\mathbf{X}}_{r,t}^{\dagger}\tilde{\mathbf{R}}_{r,t}^{-1}\tilde{\mathbf{s}}_{r,t}}{\tilde{\mathbf{s}}_{r,t}^{\dagger}\tilde{\mathbf{R}}_{r,t}^{-1}\tilde{\mathbf{s}}_{r,t}} \underset{H_0}{\overset{H_1}{\gtrless}} \xi, \tag{16}$$

where ξ is the detection threshold. Here, (16) is referred to as the MIMO-PSMI detector.

Note that Ξ in (16) is different from the test statistic in [15, eq. (13)], since the weight vectors $\mathbf{w}_{r,t}$ in (15) are distinct for different transmit-receive pairs, whereas the weight vectors in [15, eq. (13)] are all the same. Compared with the MIMO-PGLRT detector in (12), the MIMO-PSMI detector in (16) has a simpler structure. More specifically, (16) does not need to compute the term $(\mathbf{I}_2 + \tilde{\mathbf{X}}_{r,t}^{\dagger}\tilde{\mathbf{R}}_{r,t}^{-1}\tilde{\mathbf{X}}_{r,t})^{-1}$, and thus is computationally more efficient.

IV. Simulations Results

In this section, numerical simulations are conducted to validate the above theoretical analysis and illustrate the performance of the proposed two detectors. For simplicity, we consider a MIMO radar comprised of two transmit antennas and two receive antennas (i.e., $M = N = 2$), and each transmit antenna sends nine coherent pulses with equal spacing (i.e., $Q_1 = Q_2 = 9$). The steering vector $\mathbf{s}_{r,t}$ has the form as (2). Suppose further that the normalized Doppler shifts of the target are 0.1, 0.2, 0.3 and 0.4 for the (1,1), (1,2), (2,1) and (2,2) transmit-receive pairs, respectively. The (i,j)th element of the noise covariance matrix is chosen to be $[\mathbf{R}]_{i,j} = \sigma^2 0.95^{|i-j|}$, where σ^2 represents the noise power. Without loss of generality, each transmit-receive pair has the same number of secondary data which is uniformly denoted by K. $a_{r,t}$'s are also supposed to be the same, and then can be uniformly denoted by a. The signal-to-noise ratio (SNR) is defined by $\mathrm{SNR} = 10\log_{10}|a|^2/\sigma^2$.

In Fig. 1, performance comparisons among the proposed detectors and the MIMO-GLRT detector developed in [8] are presented with different K. It is shown that the performance gains of the MIMO-PGLRT detector and the MIMO-PSMI detector with respect to the MIMO-GLRT detector in the case of $K = 10$ are about 7.3 dB and 5.8 dB, respectively, when the detection probability is 0.8. In addition, the more the number

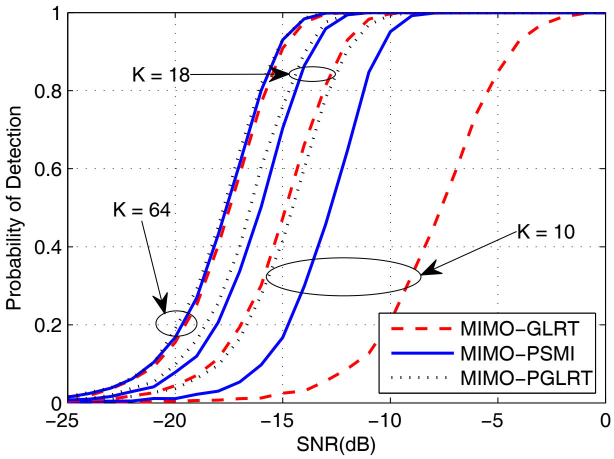

Fig. 1. Performance comparisons between three detectors with different amount of secondary data for fixed $P_{\mathrm{FA}} = 10^{-3}$. The dashed, solid, and dotted lines indicate detection probabilities obtained with Monte Carlo simulations for the MIMO-GLRT, MIMO-PSMI, and MIMO-PGLRT detectors, respectively.

of the secondary data, the better the performance. In particular, the performance difference between these detectors can be negligible in the case of sufficient secondary data (for instance, $K = 64$ in this example). This is due to the fact that using sufficient secondary data, one can obtain a high accuracy in the noise covariance matrix estimate, even without a-priori information on the persymmetric structures.

V. Conclusion

In this paper, we propose two persymmetric detectors (i.e., MIMO-PGLRT and MIMO-PSMI) in a distributed MIMO radar by exploiting persymmetric structures in received signals. The MIMO-PSMI detector has lower computational burden than the MIMO-PGLRT detector. Simulations results show that with a limited amount of secondary data, the two proposed detectors significantly outperform the conventional MIMO-GLRT detector which do not exploit the persymmetric structure, and the MIMO-PGLRT detector performs better than the MIMO-PSMI detector. When the amount of secondary data is sufficient, all detectors considered in this paper achieve similar detection performance.

Appendix A
A Derivation of MIMO-PGLRT Detector

Since the random variables $\mathbf{X}_{r,t}$ are independent, the maximization of the left-hand side of (4) can be performed term by term. Using (5), we can rewrite (4) as

$$\prod_{r=1}^{N}\prod_{t=1}^{M}\underbrace{\frac{\max_{\{a_{r,t},\mathbf{R}_{r,t}\}} f_{r,t,1}}{\max_{\{\mathbf{R}_{r,t}\}} f_{r,t,0}}}_{\triangleq \Upsilon_{r,t}} \underset{H_0}{\overset{H_1}{\gtrless}} \lambda_0. \tag{A.1}$$

Exploiting the persymmetric structure of $\mathbf{R}_{r,t}$, we have

$$\mathrm{tr}(\mathbf{R}_{r,t}^{-1}\mathbf{T}_{r,t,q}) = \mathrm{tr}(\mathbf{R}_{r,t}^{-1}\mathbf{J}\mathbf{T}_{r,t,q}^{*}\mathbf{J}). \tag{A.2}$$

Then,

$$\mathrm{tr}(\mathbf{R}_{r,t}^{-1}\mathbf{T}_{r,t,q}) = \mathrm{tr}(\mathbf{R}_{r,t}^{-1}\hat{\mathbf{T}}_{r,t,q}), \tag{A.3}$$

where

$$\hat{\mathbf{T}}_{r,t,q} = (\mathbf{T}_{r,t,q} + \mathbf{J}\mathbf{T}_{r,t,q}^{*}\mathbf{J})/2. \tag{A.4}$$

Using (7), $\hat{\mathbf{T}}_{r,t,q}$ can be rewritten as [13, eq. (A13)]

$$\hat{\mathbf{T}}_{r,t,q} = \frac{1}{K_{r,t}+1}\left[\hat{\mathbf{R}}_{r,t} + (\hat{\mathbf{X}}_{r,t} - q\,\mathbf{s}_{r,t}\hat{\mathbf{a}}_{r,t})(\hat{\mathbf{X}}_{r,t} - q\,\mathbf{s}_{r,t}\hat{\mathbf{a}}_{r,t})^{\dagger}\right], \tag{A.5}$$

where $\hat{\mathbf{a}}_{r,t} = [\mathfrak{Re}(a_{r,t}),\, \jmath\,\mathfrak{Im}(a_{r,t})]$,

$$\hat{\mathbf{R}}_{r,t} = \frac{1}{2}\sum_{k=1}^{K_{r,t}}\left\{\mathbf{y}_{r,t}(k)\mathbf{y}_{r,t}^{\dagger}(k) + \mathbf{J}[\mathbf{y}_{r,t}(k)\mathbf{y}_{r,t}^{\dagger}(k)]^{*}\mathbf{J}\right\} \tag{A.6}$$

and

$$\hat{\mathbf{X}}_{r,t} = [\hat{\mathbf{x}}_{r,t}^{\mathrm{e}}, \hat{\mathbf{x}}_{r,t}^{\mathrm{o}}] \tag{A.7}$$

with $\hat{\mathbf{x}}_{r,t}^{\mathrm{e}} = (\mathbf{x}_{r,t} + \mathbf{J}\mathbf{x}_{r,t}^{*})/2$ and $\hat{\mathbf{x}}_{r,t}^{\mathrm{e}} = (\mathbf{x}_{r,t} - \mathbf{J}\mathbf{x}_{r,t}^{*})/2$.

According to [14], the ML estimates of $\mathbf{R}_{r,t}$ under H_0 and H_1 are $\hat{\mathbf{T}}_{r,t,0}$ and $\hat{\mathbf{T}}_{r,t,1}$, respectively. Using these ML estimates, we can write $\Upsilon_{r,t}$ defined in (A.1) as

$$\Upsilon_{r,t} = \left[\frac{\det(\hat{\mathbf{T}}_{r,t,0})}{\min_{\{\hat{\mathbf{a}}_{r,t}\}}\det(\hat{\mathbf{T}}_{r,t,1})}\right]^{K_{r,t}+1}. \tag{A.8}$$

It follows from (A.5) that

$$\det(\hat{\mathbf{T}}_{r,t,1}) = \frac{1}{(K_{r,t}+1)^{Q_t}}\det(\hat{\mathbf{R}}_{r,t})\det[\mathbf{I}_2 + (\hat{\mathbf{X}}_{r,t} - \mathbf{s}_{r,t}\hat{\mathbf{a}}_{r,t})^{\dagger}\hat{\mathbf{R}}_{r,t}^{-1}(\hat{\mathbf{X}}_{r,t} - \mathbf{s}_{r,t}\hat{\mathbf{a}}_{r,t})]. \tag{A.9}$$

It is straightforward that the value of $\hat{\mathbf{a}}_{r,t}$ minimizing the denominator of (A.8) is $(\mathbf{s}_{r,t}^{\dagger}\hat{\mathbf{R}}_{r,t}^{-1}\mathbf{s}_{r,t})^{-1}\mathbf{s}_{r,t}^{\dagger}\hat{\mathbf{R}}_{r,t}^{-1}\hat{\mathbf{X}}_{r,t}$. Substituting this ML estimate into (A.8) and after some algebraic manipulations, we can obtain

$$\Upsilon_{r,t} = \left(\frac{1}{1-\Phi_{r,t}}\right)^{K_{r,t}+1}, \tag{A.10}$$

where

$$\Phi_{r,t} = \frac{\mathbf{s}_{r,t}^{\dagger}\hat{\mathbf{R}}_{r,t}^{-1}\hat{\mathbf{X}}_{r,t}(\mathbf{I}_2 + \hat{\mathbf{X}}_{r,t}^{\dagger}\hat{\mathbf{R}}_{r,t}^{-1}\hat{\mathbf{X}}_{r,t})^{-1}\hat{\mathbf{X}}_{r,t}^{\dagger}\hat{\mathbf{R}}_{r,t}^{-1}\mathbf{s}_{r,t}}{\mathbf{s}_{r,t}^{\dagger}\hat{\mathbf{R}}_{r,t}^{-1}\mathbf{s}_{r,t}}. \tag{A.11}$$

Define two unitary matrices

$$\mathbf{D} = \frac{1}{2}[(\mathbf{I}+\mathbf{J}) + \jmath\,(\mathbf{I}-\mathbf{J})] \quad \text{and} \quad \mathbf{V} = \begin{bmatrix} 1 & 0 \\ 0 & -\jmath \end{bmatrix}. \tag{A.12}$$

Then, $\Phi_{r,t}$ in (A.11) can be rewritten in the real domain as

$$\Phi_{r,t} = \frac{\tilde{\mathbf{s}}_{r,t}^{\dagger}\tilde{\mathbf{R}}_{r,t}^{-1}\tilde{\mathbf{X}}_{r,t}(\mathbf{I}_2 + \tilde{\mathbf{X}}_{r,t}^{\dagger}\tilde{\mathbf{R}}_{r,t}^{-1}\tilde{\mathbf{X}}_{r,t})^{-1}\tilde{\mathbf{X}}_{r,t}^{\dagger}\tilde{\mathbf{R}}_{r,t}^{-1}\tilde{\mathbf{s}}_{r,t}}{\tilde{\mathbf{s}}_{r,t}^{\dagger}\tilde{\mathbf{R}}_{r,t}^{-1}\tilde{\mathbf{s}}_{r,t}}, \tag{A.13}$$

where $\tilde{\mathbf{X}}_{r,t} = \mathbf{D}\hat{\mathbf{X}}_{r,t}\mathbf{V}^{\dagger}$, $\tilde{\mathbf{R}}_{r,t} = \mathbf{D}\hat{\mathbf{R}}_{r,t}\mathbf{D}^{\dagger} = \mathfrak{Re}(\hat{\mathbf{R}}_{r,t}) + \mathbf{J}\mathfrak{Im}(\hat{\mathbf{R}}_{r,t})$ and $\tilde{\mathbf{s}}_{r,t} = \mathbf{D}\mathbf{s}_{r,t} = \mathfrak{Re}(\mathbf{s}_{r,t}) - \mathfrak{Im}(\mathbf{s}_{r,t})$. Furthermore, $\tilde{\mathbf{X}}_{r,t}$ can be expressed as (11).

REFERENCES

[1] J. Li and P. Stoica, *MIMO Radar Signal Processing*. Hoboken, NJ: John Wiley & Sons, 2009.

[2] ——, "MIMO radar with colocated antennas," *IEEE Signal Processing Magazine*, vol. 24, no. 5, pp. 106–114, September 2007.

[3] H. Li and B. Himed, "Transmit subaperturing for MIMO radars with colocated antennas," *IEEE Journal of Selected Topics in Signal Processing*, vol. 4, no. 1, pp. 55–65, February 2010.

[4] A. M. Haimovich, R. S. Blum, and L. J. Cimini, "MIMO radar with widely separated antennas," *IEEE Signal Processing Magazine*, vol. 25, no. 1, pp. 116–129, January 2008.

[5] P. Wang, H. Li, and B. Himed, "Moving target detection using distributed MIMO radar in clutter with nonhomogeneous power," *IEEE Transactions on Signal Processing*, vol. 59, no. 10, pp. 4809–4820, October 2011.

[6] A. De Maio and M. Lops, "Design principles of MIMO radar detectors," *IEEE Transactions on Aerospace and Electronic Systems*, vol. 43, no. 3, pp. 886–898, July 2007.

[7] A. Sheikhi and A. Zamani, "Temporal coherent adaptive target detection for multi-input multi-output radars in clutter," *IET Radar, Sonar & Navigation*, vol. 2, no. 2, pp. 86–96, April 2008.

[8] J. Liu, Z.-J. Zhang, Y. Cao, and S. Yang, "A closed-form expression for false alarm rate of adaptive MIMO-GLRT detector with distributed MIMO radar," *Signal Processing*, vol. 93, no. 9, pp. 2771–2776, September 2013.

[9] K. F. McDonald and R. S. Blum, "Exact performance of STAP algorithms with mismatched steering and clutter statistics," *IEEE Transactions on Signal Processing*, vol. 48, no. 10, pp. 2750–2763, October 2000.

[10] V. Monga and M. Rangaswamy, "Rank constrained ML estimation of structured covariance matrices with applications in radar target detection," in *Radar Conference (RADAR), IEEE*, 2012, pp. 0475–0480.

[11] A. De Maio, "Maximum likelihood estimation of structured persymmetric covariance matrices," *Signal Processing*, vol. 83, no. 3, pp. 633–640, March 2003.

[12] H. L. Van Trees, *Optimum Array Processing, Part IV of Detection, Estimation, and Modulation Theory*. Wiley-Interscience, 2002.

[13] L. Cai and H. Wang, "A persymmetric multiband GLR algorithm," *IEEE Transactions on Aerospace and Electronic Systems*, vol. 28, no. 3, pp. 806–816, July 1992.

[14] R. Nitzberg, "Application of maximum likelihood estimation of persymmetric covariance matrices to adaptive processing," *IEEE Transactions on Aerospace and Electronic Systems*, vol. AES-16, no. 1, pp. 124–127, January 1980.

[15] L. Cai and H. Wang, "A persymmetric modified-SMI algorithm," *Signal processing*, vol. 23, no. 1, pp. 27–34, January 1991.

[16] M. Casillo, A. De Maio, S. Iommelli, and L. Landi, "A persymmetric GLRT for adaptive detection in partially-homogeneous environment," *IEEE Signal Processing Letters*, vol. 14, no. 12, pp. 1016–1019, December 2007.

[17] G. Pailloux, P. Forster, J.-P. Ovarlez, and F. Pascal, "Persymmetric adaptive radar detectors," *IEEE Transactions on Aerospace and Electronic Systems*, vol. 47, no. 4, pp. 2376–2390, October 2011.

[18] C. Hao, D. Orlando, X. Ma, and C. Hou, "Persymmetric Rao and Wald tests for partially homogeneous environment," *IEEE Signal Processing Letters*, vol. 19, no. 9, pp. 587–590, September 2012.

[19] P. Wang, Z. Sahinoglu, M.-O. Pun, and H. Li, "Persymmetric parametric adaptive matched filter for multichannel adaptive signal detection," *IEEE Transactions on Signal Processing*, vol. 60, no. 6, pp. 3322–3328, June 2012.

[20] Y. Gao, G. Liao, S. Zhu, and D. Yang, "A persymmetric GLRT for adaptive detection in compound-Gaussian clutter with random texture," *IEEE Signal Processing Letters*, vol. 21, no. 6, pp. 615–618, June 2013.